Biochimica et Biophysica Acta, 469 (1977) 311—325

BBA 77794

PHOSPHOLIPID EXCHANGE BETWEEN BILAYER MEMBRANES

GABRIELE DUCKWITZ-PETERLEIN [a], GERT EILENBERGER [a] and PETER OVERATH [b,*]

[a] *Institut für Theoretische Physik der Universität zu Köln, D5 Köln 41 and the* [b] *Max-Planck-Institut für Biologie, D74 Tübingen (G.F.R.)*

(Received January 7th, 1977)
(Revised manuscript received May 13th, 1977)

Summary

The mode of interaction of aqueous dispersions of phospholipid vesicles is investigated. The vesicles (average diameter 950 Å) are prepared from total lipid extracts of *Escherichia coli* composed of phosphatidylethanolamine, phosphatidylglycerol and cardiolipin. One type of vesicle contains *trans*-Δ^9-octadecenoate, the other type *trans*-Δ^9-hexadecenoate as predominant acyl chain component. The vesicles show order↔disorder transitions at transition temperatures, T_t = 42°C and T_t = 29°C, respectively. A mixture of these vesicles is incubated at 45°C and lipid transfer is studied as a function of time using the phase transition as an indicator. The system reveals the following properties: Lipids are transferred between the two vesicle types giving rise to a vesicle population where both lipid components are homogeneously mixed. Lipid transfer is asymmetric, i.e. *trans*-Δ^9-hexadecenoate-containing lipid molecules appear more rapidly in the *trans*-Δ^9-octadecenoate-containing vesicles than vice versa. At a given molar ratio of the two types of vesicles the rate of lipid transfer is independent of the total vesicle concentration. It is concluded that lipid exchange through the water phase by way of single molecules or micelles is the mode of communication of these negatively charged lipid vesicles.

Introduction

Which mechanisms govern the interaction of biological membranes? This basic question can be addressed to highly complex processes like cell-cell recognition and membrane fusion [1—4] or, on a somewhat lower level of sophistica-

* To whom reprint requests should be addressed.
Abbreviations: P- and E-lipids, phospholipid hydrocarbon chains containing *trans*-Δ^9-hexadecenoate and *trans*-Δ^9-octadecenoate, respectively.

tion, to the interaction of isolated membrane vesicles [5,6] or the interaction between cells and phospholipid vesicles [7—13]. Alternatively, model studies on the mode of interaction of phospholipid vesicles with defined composition should reveal some of the basic features of more complex systems. This paper is devoted to the analysis of such a model system.

A mixture of two types of phospholipid bilayer vesicles may communicate in four distinctly different ways: (1) The vesicles do not interact directly. However, since there is an equilibrium between vesicle-associated and water-dissolved phospholipid molecules, molecular exchange between the vesicles may occur through the water phase. (2) In addition to freely dissolved and vesicle-associated lipids a dispersion may always contain a small fraction of the lipids in the form of micelles. An association-dissociation equilibrium between micelles and vesicles may lead to transfer of lipids between vesicles. (3) The vesicles may exchange phospholipid molecules upon collision. (4) The vesicles may fuse upon collision giving rise to recombinant vesicles which may separate again by fission. We will designate these four mechanisms: molecular exchange, micellar exchange, collision-exchange and fusion, respectively. Provided that the lipid species are miscible, all four mechanisms will eventually lead to a homogeneously mixed vesicle population.

The mechanism(s) and kinetics of vesicle interaction will depend on the following parameters: the structure of the phospholipids and their critical micellar and "critical bilayer" concentration (cf. mechanisms 1 and 2, respectively), the size and concentration of vesicles, variables such as pH, ionic strength, and temperature as well as the presence or absence of other lipidic or non-lipidic components. In view of the large number of variables no rules have emerged as to which mechanism of interaction will dominate the events under a given set of conditions [14—23].

In the present study, we chose to investigate the interaction of bilayer vesicles formed from total phospholipid extracts of the bacterium *Escherichia coli.* The lipids contain about 80% of the zwitter-ionic phosphatidylethanolamine and 20% of the acidic lipids phosphatidylglycerol and cardiolipin. Vesicles formed from these lipids will thus be negatively charged in the neutral pH region. It will be shown that exchange of molecules through the water phase by way of single molecules or micelles appears to be the predominant mode of communication of such vesicles.

Lipid exchange will be analyzed using two vesicle populations having a different phospholipid hydrocarbon chain composition. One type contains *trans*-Δ^9-hexadecenoate, the other *trans*-Δ^9-octadecenoate as predominant fatty acid. The lipids will be referred to as P-lipids and E-lipids, respectively. Aqueous dispersions of P- and E-lipids show order↔disorder phase transitions at distinct temperatures [24] which serve as the tool for analyzing the mechanism of lipid transfer.

Materials and Methods

Phospholipids. The lipid samples used in this study were isolated from the unsaturated fatty acid-requiring *E. coli* mutant strain K1062. Their preparation and properties have been described in detail in a previous communication

[24]. Total lipid extracts from whole cells grown in the presence of *trans*-Δ^9-$C_{18:1}$ * or *trans*-Δ^9-$C_{16:1}$ were fractionated by silicic acid chromatography and all phospholipid-containing fractions were pooled. The samples contained 82 mol % phosphatidylethanolamine, 11 mol % cardiolipin and 7 mol % phosphatidylglycerol as determined for a representative sample of E-lipid extract. The fatty acid composition of the E-lipids (in mol %) was: $C_{12:0}$ = 1.6, $C_{14:0}$ = 14.0, $C_{16:0}$ = 13.5, $C_{16:1}$ = 2.6, *trans*-Δ^9-$C_{18:1}$ = 68.3. The P-lipids contained $C_{14:0}$ = 4.3, $C_{16:0}$ = 12.8, *trans*-Δ^9-$C_{16:1}$ = 82.8. The average molecular weight was 809 and 760 for the E- and P-lipids, respectively.

10 mg lipid in 4 ml bidistilled water were sonicated for 10 min at 45°C under nitrogen using a Branson Sonifier at a power setting of 30 W. The dispersions were diluted to a concentration of $2 \cdot 10^{-3}$ M and incubated for 12 h at 45°C. The transition temperature of E- and P-lipids remained unaffected by incubation times up to 60 h. This is taken as evidence that lipid breakdown is negligible under these conditions. The samples had a pH 5.5—5.8.

Electronmicroscopy of highly diluted lipid dispersions (10^{-8} M) was performed by the agar filtration technique described by Kellenberger and Arber [25]. In this technique, the vesicles are filtered onto a collodium film which covers the surface of an agar plate. The collodium film is subsequently transferred to a grid and shadowed with platinum. The diameter of the vesicles is taken from electron micrographs of the platinum replicas.

Measurement of lipid phase transitions. These were monitored by 90° light scattering in a Hitachi-Perkin-Elmer Model MPF3 spectrofluorimeter at a wavelength of 400 nm for both excitation and emission as previously described [24]. The temperature in the cuvet was changed between 20 and 50°C at a rate of 1°C/min.

Normalization of the transition curves. Above and below the transition (cf. Fig. 2) the curves show a non-linear decrease in intensity (I) as a function of temperature (T), which can be described by an exponential function of the form

$$n_{1,2}(T) = a \cdot e^{-bT} + c_{1,2} \tag{1}$$

The indices 1 and 2 refer to the low-temperature and the high-temperature part of the curves, respectively. The functions $n_{1,2}(T)$ were extrapolated to the temperature range of the transition. Choosing $n_2(T)$ as base line, a normalized transition curve $N(T)$ between 0 and 1 was obtained:

$$N(T) = \frac{I(T) - n_2(T)}{c_1 - c_2} \tag{2}$$

The same procedure was applied to composite curves of mixtures of two lipid components (cf. Figs. 2 and 3).

Numerical fitting of the transition curves. The normalized transition curves were numerically fitted to an empirical function. For single components E or P (cf. Fig. 2B) a modified hyperbolic tangens of the following form was used

$$f_{E,P}(T) = 1/2[1 - \tanh\{S_{E,P}(T - T_{t_{E,P}}) + k(T - T_{t_{E,P}})^3\}] \tag{3}$$

* Fatty acids are designated by the number of carbon atoms before the colon and the number of double bonds after the colon.

S denotes the slope of the curve. The transition temperature, T_t, is defined as the point of inflection of the curve. The third-order term $k\ (T-T_{t_{E,P}})^3$ was introduced in order to describe the sharp shoulders of the curves. Fitting of the single component curves yielded a value for $k = 0.006$. This value was subsequently also used for composite curves obtained for mixtures of E- and P-vesicles.

In composite curves of two vesicle populations (cf. Fig. 3B) $f(T)$ can be described by the sum of the two components

$$f(T)_{E+P} = 1/2A_P[Z_P] + 1/2(1 - A_P)[Z_E] \quad (4)$$

Here Z_P and Z_E refer to the term in brackets in Eqn. 3 for the E- and P-component, respectively. A_P and $A_E = 1-A_P$ denote the amplitudes of the two components.

Eqn. 4 was used to determine the free parameters A_P, S_E, S_P, T_{t_E}, and T_{t_P} by fitting the function $f(T)_{E+P}$ to the normalized curves using a chi-square-fit.

Results

Properties of lipid vesicles

Size distribution. The size distribution of the lipid vesicles used in this study is shown in Fig. 1. The average diameter, $\bar{d}$, for the E-vesicles is 950 Å. Within the experimental error, $\bar{d}$ did not change when the vesicles were incubated for 4800 min at 45° C. Moreover, the size distribution of an equal mixture of E- and P-vesicles is similar directly after mixing and after 2400 min at 45° C. Thus, the size distribution appears to be in a state of equilibrium. However, this constancy could either indicate that the vesicles do not interact at all or it could be maintained in spite of the occurrence of complex fusion/fission or exchange processes.

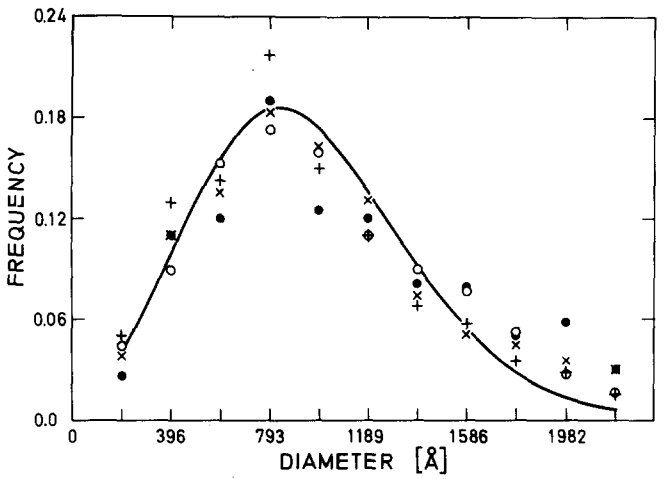

Fig. 1. Size distribution of lipid vesicles. Vesicle sizes were divided into classes. The figure shows the normalized frequency as a function of the diameter of the vesicle classes. ●, E-vesicles at $t = 0$ min and +, after 4800 min at 45°C, $c = 2 \cdot 10^{-3}$ M; X, equimolar mixture of E- and P-vesicles at $t = 0$ and ○, after 2400 min at 45°C, $c = 2 \cdot 10^{-3}$ M. The curve gives the theoretical size distribution for an average diameter $\bar{d} = 950$ Å assuming a Poisson distribution, since $d-\bar{d}$ is comparable to $\bar{d}$.

Lipid phase transitions of the individual components. E- and P-vesicles reveal reversible changes in 90° light scattering intensity at the order↔disorder transition (cf. Fig. 2A and ref. 24). On a molar basis, the change in intensity at the phase transition is smaller for P-vesicles than for E-vesicles. The rising temperature scans were normalized and fitted to an empirical formula (see Eqn. 3 in Materials and Methods). Fig. 2B shows the agreement between the experimental and the computer simulated curves. Values for the transition temperatures are $T_{t_P} = 29°\,C$ and $T_{t_E} = 42°\,C$ for the P- and E-vesicles, respectively.

In a mixture of vesicles the light scattering characteristics of the individual components are retained and can be described by the following additive function:

$$rI(T)_E + (1 - r)I(T)_P = I(T)_{E+P}\,. \tag{5}$$

$I(T)_E$, $I(T)_P$ and $I(T)_{E+P}$ denote the scattering intensity as a function of temperature for the single components and the mixture, respectively. The mol fraction of the vesicle mixture, r, is defined as

$$r = \frac{[E]}{[E] + [P]} \tag{6}$$

where $[E]$ and $[P]$ denote the concentration of E- and P-lipids, respectively.

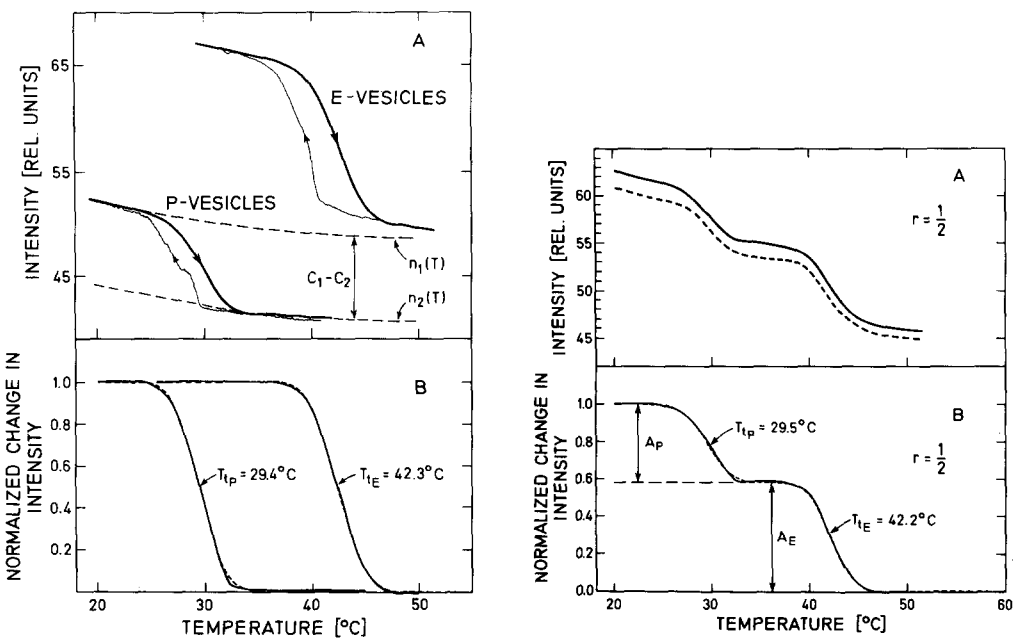

Fig. 2. Lipid phase transition of E- or P-lipid vesicles. (A) Change in 90° light scattering intensity of E- or P-lipid vesicles, $c = 2 \cdot 10^{-4}$ M. Arrows refer to direction of temperature scan. (B) Normalized change in scattering intensity (———) for rising temperature scans. The dashed curves (- - - - -) are computer simulated (cf. Eqn. 3).

Fig. 3. Lipid phase transition of a mixture of E- and P-lipid vesicles. (A) Change in 90° light scattering intensity of an equimolar mixture of E- and P-lipid vesicles, total lipid concentration, $c = 2 \cdot 10^{-4}$ M. The dashed curve was calculated from the individual components (cf. Fig. 2) using Eqn. 5. (B) Normalized curve (———) and computer simulated curve using Eqn. 4 (- - - - -).

For a given value of r, $I(T)_{E+P}$ remained constant throughout an exchange experiment (cf. Fig. 5) both for $T \gg T_{t_E}, T_{t_P}$ or $T \ll T_{t_E}, T_{t_P}$.

In Fig. 3A an experimental curve $I(T)_{E+P}$ for an equimolar mixture of vesicles ($r = 1/2$) is compared with a curve calculated from $I(T)_E$ and $I(T)_P$ (cf. Fig. 2A) according to Eqn. 5. Since the E- and P-vesicles evidently contribute to the total light scattering intensity in an additive way, the characteristics of the two components regarding both the values for the transition temperature, T_{t_P} and T_{t_E}, as well as their relative contribution to the amplitudes of the intensity change at the transition, A_E and A_P, are retained after normalization (cf. Fig. 3B).

Phase diagram of lipid mixtures. Lipid exchange between E- and P-vesicles will be analyzed in terms of changes in the transition temperatures, $T_{t_{E,P}}$ and changes in the amplitudes, $A_{E,P}$. Therefore, it was important to study the behaviour of homogeneous mixtures of the two components. E- and P-lipids were dissolved in benzene and mixed in various proportions. After removal of the solvent, aqueous dispersions were prepared by sonication and analyzed by 90° light scattering. Fig. 4A demonstrates that the T_t values of mixed vesicles fall on a straight line between the extremes, T_{t_P} and T_{t_E}, i.e.

$$T_t(x) = (T_{t_E} - T_{t_P})x + T_{t_P} \tag{7}$$

where x refers to the molar ratio of E-lipids in the mixed vesicle population. This result suggests that E- and P-lipids are completely miscible at all values of x

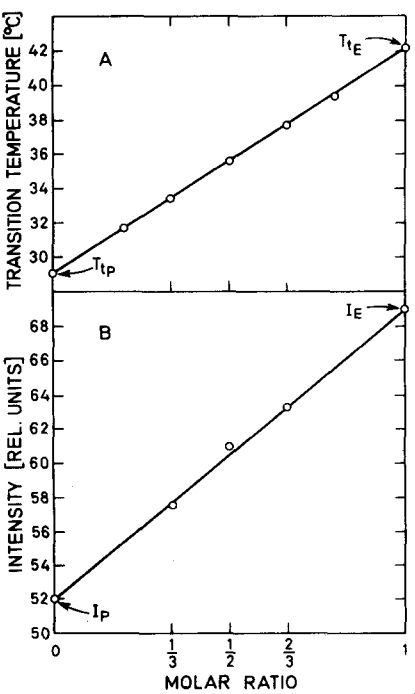

Fig. 4. Transition temperature (A) and 90° light scattering intensity (B) as a function of the molar ratio, x. Total lipid concentration, $c = 2 \cdot 10^{-4}$ M. The values in B refer to $T = 20°C$. See text for further details.

both in the ordered and fluid states as expected from previous in vivo experiments [26].

Provided that the vesicle size distribution is the same (cf. Fig. 1), it may be assumed that the difference in the light scattering intensity, I, observed for P- and E-vesicles (cf. Fig. 2A) is a characteristic property of the P- and E-lipid molecules themselves. This view is supported by the diagram shown in Fig. 4B. By plotting the intensity of mixed vesicles as a function of x, a straight line is obtained between the extremes I_E and I_P for the single component vesicles. It thus appears that each lipid molecule contributes specifically to the total scattering intensity.

Analysis of lipid exchange

Kinetics. Aqueous dispersions of E- and P-vesicles, preequilibrated by incubation for 12 h at 45°C, were mixed at a molar ratio, $r = 1/2$, and a total lipid concentration, $c = 2 \cdot 10^{-3}$ M. The mixture was incubated at 45°C, i.e. at a temperature, $T_{t_P} \ll T > T_{t_E}$, where the lipids in both types of vesicles are in a fluid state. At various times, samples were analyzed by 90° light scattering and the rising temperature scans were normalized as described above.

It is immediately clear from the representative curves shown in Fig. 5 that E- and P-vesicles interact and eventually give rise to a population of mixed vesicles characterized by a single transition with a transition temperature, $(T_{t_{E+P}})_{r=1/2} =$ 36°C (compare Fig. 4A). The two transitions gradually merge indicating lipid transfer in both directions. The two arising mixed vesicle populations will be designated I and II, i.e. type I-vesicles are formed from P-vesicles by incorporation of E-molecules and type II-vesicles are formed from E-vesicles by incorporation of P-molecules.

The function $f(T)$ (cf. Eqn. 4 for P ≡ I and E ≡ II) can be fitted to the experimental curves with a remarkable degree of accuracy (compare dashed and

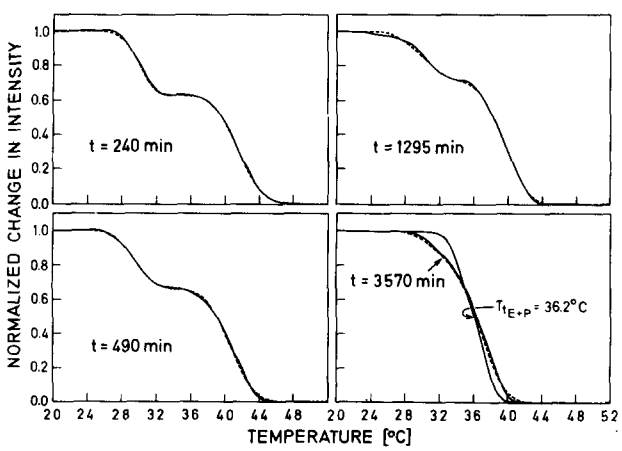

Fig. 5. Kinetics of lipid exchange. E- and P-lipid vesicles were mixed at a molar ratio, $r = 1/2$, and a total concentration $c = 2 \cdot 10^{-3}$ M. The mixture was incubated at 45°C. At the times indicated, samples were diluted 10-fold and analyzed by 90° light scattering. Solid lines refer to experimental (normalized rising temperature scans), dashed lines to computer simulated curves. The control curve at $t = 0$ is shown in Fig. 3B. The curve with $T_{t_{E+P}}$ corresponds to a homogeneously mixed vesicle preparation at $x = 1/2$, cf. Fig. 4A.

solid lines in Fig. 5). This suggests that throughout the mixing process the dispersion can be considered to be composed of only two vesicle populations, I and II. As discussed below, this behaviour argues strongly against vesicle fusion as a mechanism of lipid mixing.

Vesicle populations I and II can be defined by respective values for the transition temperature $T_{t_{I,II}}$ and the amplitude $A_{I,II}$ which are obtained from the fitted curves such as those shown in Fig. 5. This evaluation of the curves implies that in the type I- and type II-vesicle populations the P- and E-molecules can be considered to be homogeneously mixed in the way discussed above for Fig. 4. $T_{t_{I,II}}$ define the composition of the two populations, while $A_{I,II}$ are a measure of the amount of lipid present in each population. In Figs. 6B and 7B $T_{t_{I,II}}$ and $A_{I,II}$ are plotted as a function of time. Clearly, for $t \to \infty$ T_{t_I} and $T_{t_{II}}$ become equal to $T_{t_{E+P}}$, i.e. $x_I = x_{II} = r$.

$T_{t_{I,II}}$ and $A_{I,II}$ can be used to calculate the number of molecules in the two vesicle populations as a function of time. The molar ratios x_I and x_{II} are related to the transition temperature (Eqn. 7) as follows:

$$x_I = \frac{T_{t_I} - T_{t_P}}{T_{t_E} - T_{t_P}} = \frac{[E]_I}{[P]_I + [E]_I} \tag{8}$$

$$x_{II} = \frac{T_{t_{II}} - T_{t_P}}{T_{t_E} - T_{t_P}} = \frac{[E]_{II}}{[P]_{II} + [E]_{II}} \tag{9}$$

where $[E]_{I,II}$ and $[P]_{I,II}$ denote the concentration of molecules in the respective vesicle population.

Mass conservation requires that

$$\frac{[P]_I + [P]_{II}}{[E] + [P]} = 1 - r \tag{10}$$

and

$$\frac{[E]_I + [E]_{II}}{[E] + [P]} = r \tag{11}$$

The continuous change of T_{t_I} and $T_{t_{II}}$ was first described by approximating the experimental values to an exponential function. This function was subsequently used to calculate $[E]_{I,II}$ and $[P]_{I,II}$ as a function of time using Eqns. 8—11. The result is shown in Fig. 8B.

The time course of $[E]_{I,II}$ and $[P]_{I,II}$ can be used to calculate the expected values for A_I and A_{II} since each E- and P-molecule contributes specifically to the amplitude in both populations:

$$A_I = [P]_I \frac{A_P}{1 - r} + [E]_I \frac{A_E}{r} \tag{12}$$

$$A_{II} = [P]_{II} \frac{A_P}{1 - r} + [E]_{II} \frac{A_E}{r} \tag{13}$$

In Fig. 7B the solid lines show the calculated time course of $A_{I,II}$. The remarkable agreement between calculated and experimentally determined amplitudes

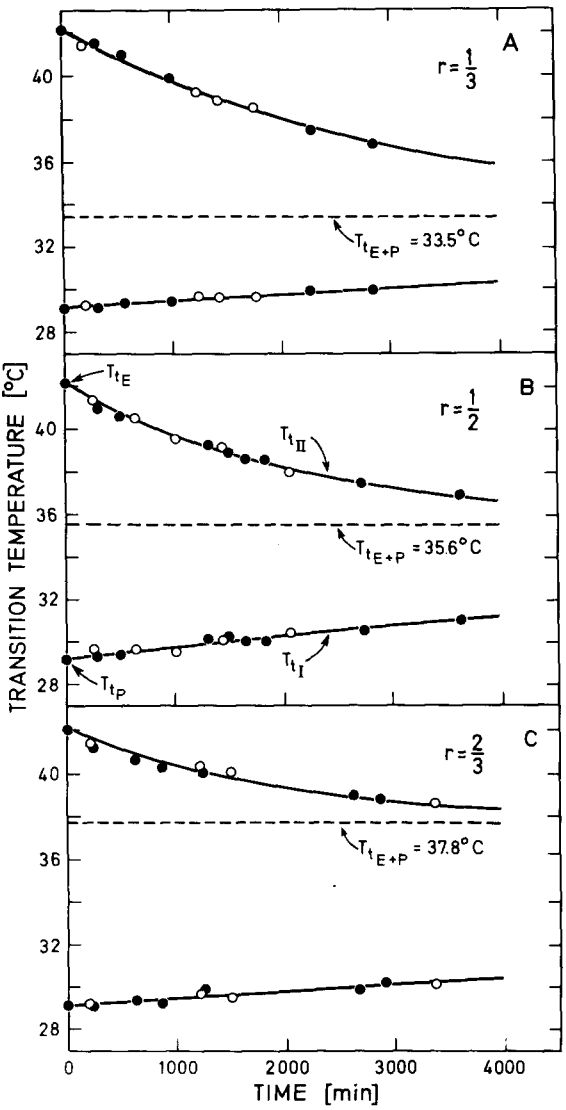

Fig. 6. Transition temperature as a function of time for $r = 1/3$ (A), $r = 1/2$ (B) and $r = 2/3$ (C) and a total lipid concentration $c = 2 \cdot 10^{-3}$ M (●) or $c = 2 \cdot 10^{-4}$ M (○); temperature of the exchange experiments, $T = 45°C$. The solid lines represent an optimal fit through the experimental values assuming an exponential change of $T_{t_{I,II}}$ with time. The horizontal dashed lines indicate the T_t values for a homogeneous mixture of E- and P-lipids at the respective value of r.

shows that the whole analysis is self-consistent.

It is evident from Fig. 8B that lipid exchange is asymmetric, i.e. transfer of P-molecules to E-vesicles is faster than transfer of E-molecules to P-vesicles. This leads to a decrease of the total amount of lipid molecules in population I and a corresponding increase in population II. Extrapolation according to an exponential time course beyond the time covered by the experiments ($t > 3600$ min) suggests that population I will disappear. Because population I will at all times have a higher percentage of the faster exchanging P-component, i.e. a higher ratio $[P]/([E] + [P])$, than population II, the total amount of lipid in

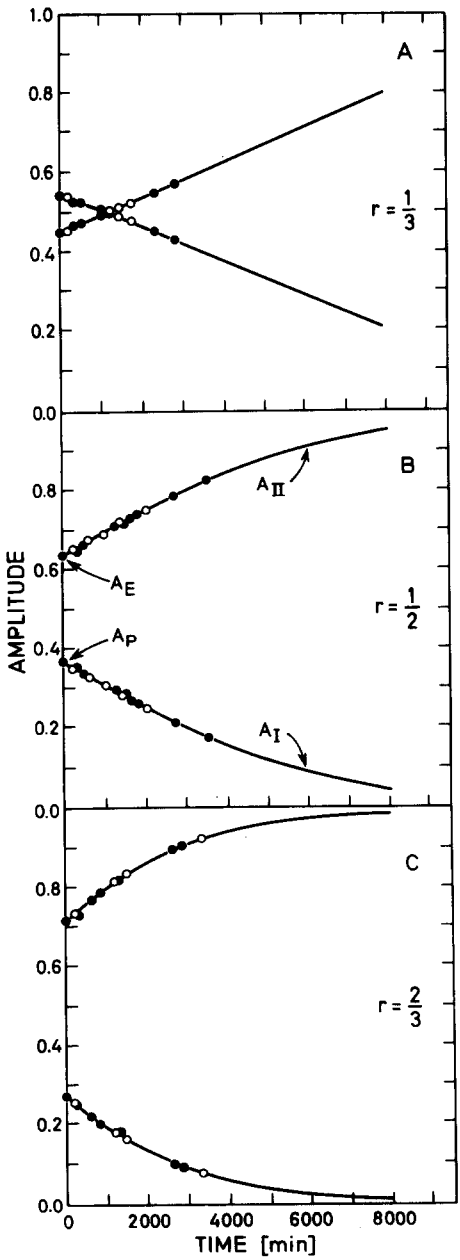

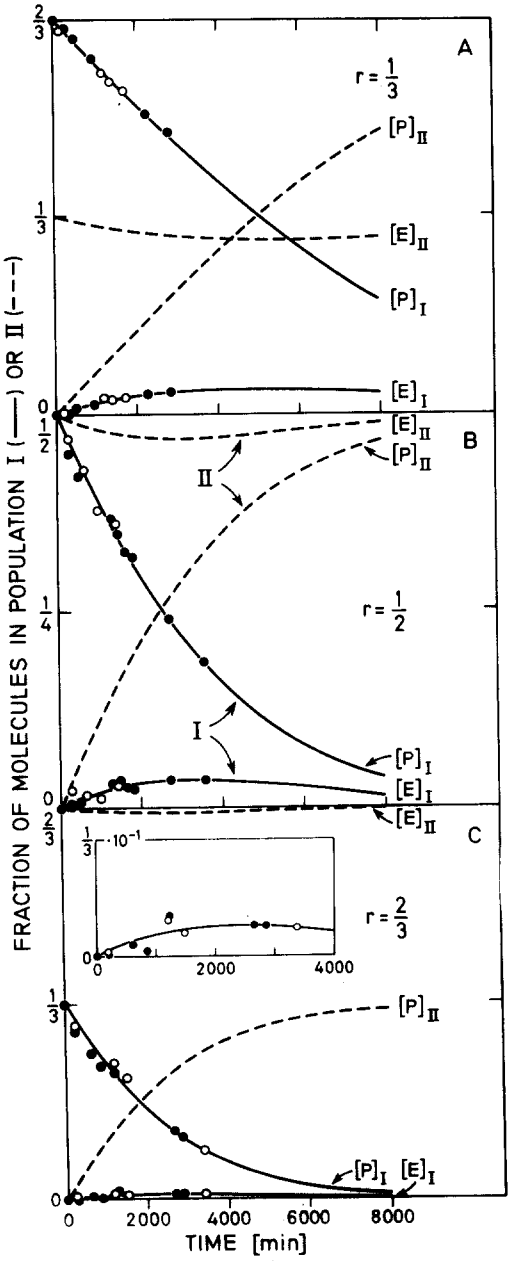

Fig. 7. Amplitudes as a function of time for $r = 1/3$ (A), $r = 1/2$ (B) and $r = 2/3$ (C). The curves are calculated from $T_{t_I}(t)$ and $T_{t_{II}}(t)$; see text for explanation.

Fig. 8. Fraction of molecules in vesicle populations I and II as a function of time as calculated from the experiments shown in Fig. 6. The time course has been extrapolated beyond that determined by experiment (compare Fig. 7). The inset in C shows the time course of $[E]_I$ on an expanded scale.

population I will decrease continuously. This implies that $[E]_I$ passes through a maximum. The time course of $[E]_I$ in Fig. 8B (see also inset to Fig. 8C) is consistent with this suggestion (see also Discussion).

Dependence on molar ratio. A kinetic analysis similar to that shown for $r = 1/2$ has been performed for molar ratios, $r = 1/3$ and $r = 2/3$. The results are plotted in the upper (A) and lower parts (C) of Figs. 6—8. Worthy of note, the rate of lipid transfer was found to be dependent on r. As a measure of this dependence one can compare the times, $t_{1/2}$, when half of the P-molecules have left population I, i.e. at $[P]_I = [P]_{II}$ (cf. Fig. 8). $t_{1/2}$ was found to have values of 5000, 2550 and 1800 min for $r = 1/3$, $1/2$ and $2/3$, respectively. Therefore, the rate of transfer of lipids from donor to receptor vesicles becomes faster as the receptor vesicle concentration is increased.

Concentration dependence. The rate of lipid transfer between the vesicles is independent of the total lipid concentration. This is evident from Figs. 6 and 7 where the filled and open circles refer to experiments at a total lipid concentration of $2 \cdot 10^{-3}$ and $2 \cdot 10^{-4}$ M, respectively. This result provides a clearcut argument for exchange through the aqueous phase as the mechanism of lipid exchange. Both collision-exchange and fusion are expected to show second or higher order kinetics.

Temperature dependence. The experiments described so far were all performed at 45° C, i.e. a temperature above the order ↔ disorder transition of both components (of Fig. 2B). It appeared of interest to study the influence of the physical state of the lipid vesicles on the exchange process. If the two vesicle populations are incubated at $T = 20°C$, i.e. below the transition of both components, $T < T_{t_P} < T_{t_E}$, or at $T = 36.5°C$, i.e. at a temperature where only the P-vesicles are in a fluid state, $T_{t_P} < T < T_{t_E}$ no discernible change in $A_{E,P}$ and $T_{t_{P,E}}$ occurred within 1700 min. These observations appear reasonable, because the decrease in mobility of lipid molecules in the ordered state will greatly reduce the probability for lipids to enter or escape from the bilayer.

In view of the proposed maximum of lateral compressibility and associated fluctuations in packing and density of lipid molecules within the range of the thermal transition [20,27] it was more interesting to study the exchange at a temperature, $T = T_{t_E} > T_{t_P}$, where ordered and fluid domains coexist in the E-vesicles. The E- and P-lipids used for these experiments had transition temperatures $T_{t_E} = 37.1°C$ and $T_{t_P} = 29.8°C$, respectively. After an incubation time, $t \approx 1000$ min, the change in amplitude, $\Delta A_{E,P}$ was about twice as high for the sample incubated at 45° C than that incubated at 37° C. Thus, the rate of lipid transfer is decreased, when the available surface area of fluid E-lipids is reduced, i.e. the experimental situation corresponds to an effective decrease in r.

Discussion

The lipid vesicles used in this study are negatively charged. They have a broad size distribution and are, on the average, large enough so that the surface curvature is not expected to cause any strain on the lipid molecules on either side of the bilayer. According to these criteria the system provides a fairly realistic model for the behaviour of the lipid part of negatively charged bilayer membranes in vivo.

The experiments reveal the following distinctive features of the system: Firstly, the rate of exchange is independent of the vesicle concentration

between a total lipid concentration of $2 \cdot 10^{-4}$ and $2 \cdot 10^{-3}$ M. Secondly, at any given time throughout the exchange, the transition curves can be considered to be composed of two populations of vesicles with respective transition temperatures and amplitudes. Either of these parameters can be used to calculate the composition of the two populations as a function of time.

These results can be interpreted in terms of the mechanisms of vesicle-vesicle interaction considered in the introductory part of this paper. Fusion of vesicles is expected to show a quadratic dependence of the vesicle concentration. Furthermore, fusion of P- and E-vesicles would give rise to hybrid vesicles having an intermediate T_t value. These hybrid vesicles could subsequently fuse again with P- and/or E-vesicles, etc. This mechanism would rapidly lead to a single broad transition instead of the two distinct transitions observed in Fig. 5. Extensive fusion would also cause a significant change in the size distribution of the vesicles which is not observed (cf. Fig. 1). Therefore, the experimental facts appear to rule out fusion as a prevailing mechanism of vesicle-vesicle interaction. The absence of vesicle fusion is in accordance with the inability of intact membrane vesicles of *E. coli* to fuse upon mere incubation [5].

Collision-exchange is likewise expected to show a quadratic dependence on the vesicle concentration. Therefore, such a mechanism appears to be inconsistent with the observed concentration independence.

The two remaining mechanisms, molecular and/or micellar exchange, suppose the transfer of lipid molecules through the water phase. Regarding the first mechanism, the presence of an extremely low but constant concentration of water-dissolved free lipid molecules is generally assumed above the critical micellar concentration. On the other hand, there is to our knowledge only very limited evidence for the presence of a likewise constant and low concentration of small lipid micelles above, what may be called the critical bilayer concentration [34]. Lipid exchange by both mechanisms is expected to be concentration independent and either mechanism is consistent with the kinetics of mixing observed in Figs. 5—7. A differentiation between these mechanisms is beyond the resolving power of our approach.

Beyond these qualitative conclusions, a quantitative analysis of the exchange kinetics revealed the following distinctive features: Firstly, the total amount of lipids in population II increases, i.e. the exchange of lipids is asymmetric. Secondly, transfer of P-lipids to population II occurs faster for increasing values of r. These observations allow a kinetic interpretation in terms of a rate constant, k_-, for the escape of lipid molecules from the bilayer surface (see accompanying paper [37] by L. Thilo).

Lipid exchange has been followed for approx. 3500 min (cf. Figs. 6B and 7B). At this time about half of the P-molecules have left vesicle population I. At the same time population I has received about 10% of the E-lipid molecules (Fig. 8). Thus, the average diameter of the type I-vesicles will have decreased by about 25% while the average diameter of the E-vesicles will have increased by about 20%. These changes are too small to cause a discernible effect on the size distribution within the experimental accuracy (cf. Fig. 1).

As discussed with reference to Figs. 7 and 8, extrapolation of the data assuming an exponential time dependence of T_t (cf. Fig. 6) leads to the conclusion that, eventually, the population I will disappear completely because all

P-molecules will have been incorporated into population II. However, as the type I-vesicles decrease in size the increase in surface energy will counteract further shrinking. Therefore, these vesicles may simply exchange E- and P-lipids without alteration of size.

It should be noted that our analysis of the mixing process assumes an equal distribution of the exchanged molecules to both sides of the bilayer. Support for this assumption comes from an analysis of the slope of the transition curves at the transition temperature, S_{T_t} (cf. Eqn. 4). Within the experimental accuracy, the slope, $S_{T_t} = 0.4 \pm 0.08$ (maximum deviation of the mean) is the same for E-, P-, type II-, and type I-vesicles as well as for homogeneously mixed vesicles at various values of r. If the distribution of E- and P-lipids in the I- and II-vesicle populations would be grossly asymmetric, we would expect a broadening of the transition, i.e. a decrease in S_{T_t} as a function of time because the two halves of the bilayer are not expected to undergo separate order↔disorder transitions. In the system considered here, a net transfer of P-lipids occurs from the P- to the E-vesicles. Thus, the outer leaflet of the receptor lipid bilayer will expand. At the same time, the bilayer will become asymmetric with regard to the lipid hydrocarbon chain composition. If the rate of flip-flop of lipid molecules between the two sides of the bilayer is fast compared to the exchange rate an asymmetric lipid distribution cannot be maintained. Half times for lipid flip-flop in 300 Å diameter, single walled phosphatidylcholine vesicles are of the order of $\geqslant$10 days [28—30]. The rate of flip-flop for the lipids used in this study is unknown. It is possible, for instance, that some minor impurity in the *E. coli* lipid extracts catalyses the equilibration of lipids across the bilayer.

It is difficult to compare the results presented in this report with a number of related studies which have concentrated largely on the behaviour of dispersions of phosphatidylcholine vesicles. Under certain conditions, such vesicles appear to undergo a rapid fusion process (half time $\tau < 1$ h) which is accelerated by impurities such as free fatty acids and is fastest near the transition temperature, T_t [15,19,22,31]. However, once "annealed" by incubation above the transition temperature, phosphatidylcholine vesicles appear to be stable for extended times ($\tau > 12$ h; cf. refs. 31 and 32). The latter type of preparation was recently analyzed by Martin and MacDonald [22] in a study of lipid exchange between dimyristoyl phosphatidylcholine and dipalmitoyl phosphatidylcholine vesicles. Using a similar experimental approach as taken in this study their system reveals striking similarities to the *E. coli* system: Transfer of lipids occurs exclusively from dimyristoyl to dipalmitoyl phosphatidylcholine vesicles (half time τ approx. 6 h). It occurs most rapidly at a temperature where both lipid components are in a fluid state. Finally, the arising mixed vesicle population shows a well defined ordered↔fluid transition suggesting a symmetrical distribution of the transferred dimyristoyl phosphatidylcholine molecules to both sides of the bilayer. Similar features of lipid mixing are revealed by the recent study of Sengupta et al. [33]. In our view, exchange through the aqueous phase appears to be the most likely mechanism of lipid transfer in all these cases.

Transfer of lipid molecules through the water phase is a basic phenomenon of membrane-membrane interaction. It is expected to occur between surface

membranes of eucaryotic cells in tissue culture or in intact tissues in vivo as well as between different membrane systems within a single cell. Although a slow process, lipid exchange tends to randomize the lipid composition of different membranes in a time scale of days. Its functional significance for membrane dynamics remains to be determined. In comparison to more effective ways of membrane interaction such as fusion and protein-catalyzed lipid exchange (see refs. 35 and 36 for review) spontaneous lipid exchange, as analyzed here for a model system, may only constitute the background noise of membrane communication.

Acknowledgements

We thank H. Würz for some preliminary experiments at the beginning of this work and H. Schwarz and H. Frank for the electron microscopic examination of our samples. We would also like to acknowledge gratefully numerous helpful discussions with L. Thilo, S. Duckwitz and E. Sackmann.

References

1 Moscona, A.A. (1974) The cell surface in development, Wiley and Sons, New York
2 Turner, R.S. and Burger, M.M. (1973) in Ergebnisse der Physiologie, Biologischen Chemie und experimentellen Pharmakologie (Adrian, R.H., et al., eds.), Vol. 68, pp. 121—155, Springer Verlag, Heidelberg
3 Poste, G. and Allison, A.C. (1973) Biochim. Biophys. Acta 300, 421—465
4 Satir, B. (1975) Sci. Am. 233, No. 4, 29—37
5 Devor, K.A., Teather, R.M., Brenner, M., Schwarz, H., Würz, H. and Overath, P. (1976) Eur. J. Biochem. 63, 459—467
6 Miller, C. and Racker, E. (1976) J. Membrane Biol. 26, 319—333
7 Grant, C.W.M. and McConnell, H.M. (1973) Proc. Natl. Acad. Sci. U.S. 70, 1238—1240
8 Pagano, R.E., Huang, L. and Wey, C. (1974) Nature 252, 166—167
9 Papahadjopoulos, D., Poste, G. and Schaeffer, B.E. (1973) Biochim. Biophys. Acta 323, 23—42
10 Martin, F. and MacDonald, R.C. (1974) Nature 252, 161—163
11 Martin, F.J. and MacDonald, R.C. (1976) J. Cell Biol. 70, 515—526
12 Huang, L. and Pagano, R.E. (1975) J. Cell Biol. 67, 38—48
13 Pagano, R.E. and Huang, L. (1975) J. Cell Biol. 67, 49—60
14 Taupin, C. and McConnell, H.M. (1972) in Mitochondria and Biomembranes (van den Bergh, S.G., Borst, P., Slater, E.C., van Deenen, L.L.M., Riemesma, J.C. and Tager, J.M., eds.), Vol. 28, pp. 219—229, North-Holland Publ. Co., Amsterdam
15 Prestegard, J.H. and Fellmeth, B. (1974) Biochemistry 13, 1122—1126
16 Papahadjopoulos, D., Poste, G., Schaeffer, B.E. and Vail, W.J. (1974) Biochim. Biophys. Acta 352, 10—28
17 Barsukov, L.I., Shapiro, Yu.E., Viktorov, A.V., Volkova, V.I., Bystrov, V.F. and Bergelson, L.D. (1974) Biochem. Biophys. Res. Commun. 60, 196—203
18 Maeda, T. and Ohnishi, S. (1974) Biochem. Biophys. Res. Commun. 60, 1509—1516
19 Kantor, H.L. and Prestegard, J.H. (1975) Biochemistry 14, 1790—1795
20 van der Bosch, J. and McConnell, H.M. (1975) Proc. Natl. Acad. Sci. U.S. 72, 4409—4413
21 Lau, A.L.Y. and Chan, S.I. (1975) Proc. Natl. Acad. Sci. U.S. 72, 2170—2174
22 Martin, F.J. and MacDonald, R.C. (1976) Biochemistry 15, 321—327
23 Dawidowicz, E.A. and Rothman, J.E. (1976) Biochim. Biophys. Acta 455, 621—630
24 Overath, P. and Träuble, H. (1973) Biochemistry 12, 2625—2634
25 Kellenberger, E. and Arber, W. (1957) Virology 3, 245—255
26 Thilo, L. and Overath, P. (1976) Biochemistry 15, 328—334
27 Linden, C.D., Wright, K.L., McConnell, H.M. and Fox, C.F. (1973) Proc. Natl. Acad. Sci. U.S. 70, 2271—2275
28 Rothman, J.E. and Dawidowicz, E.A. (1975) Biochemistry 14, 2809—2816
29 Johnson, L.W., Hughes, M.E. and Zilversmit, D.B. (1975) Biochim. Biophys. Acta 375, 176—185
30 Roseman, M., Litman, B.J. and Thompson, T.E. (1975) Biochemistry 14, 4826—4830
31 Lawaczeck, R., Kainosho, M., Girarded, J. and Chan, S.J. (1975) Nature 256, 584—586

32 Marsh, D., Watts, A. and Knowles, P.F. (1976) Biochemistry 15, 3570—3578
33 Sengupta, P., Sackmann, E., Kühnle, E. and Scholz, H.P. (1976) Biochim. Biophys. Acta 436, 869—878
34 Lawaczeck, R., Blackman, R. and Kainosho, M. (1977) Biochim. Biophys. Acta 468, 411—422
35 Bruckdorfer, K.R. and Graham, J.M. (1976) in Biological Membranes (Chapman, D. and Wallach, D.F.H., eds.), Vol. 3, pp. 103—152, Academic Press, London
36 Wirtz, K.A. (1974) Biochim. Biophys. Acta 344, 95—117
37 Thilo, L. (1977) Biochim. Biophys. Acta 469, 326—334